

Equilibrium properties of magnetic filament suspensions

Andrey A. Kuznetsov^{a,b,*}

^a*Institute of Continuous Media Mechanics UB RAS, Ac. Koroleva st. 1, 614013, Perm, Russia*

^b*Perm State University, Bukireva st. 15, 614990, Perm, Russia*

Abstract

Langevin dynamics is used to study equilibrium properties of the suspension of magnetic filaments (chains of nanoparticles permanently crosslinked with polymers). It is shown that the filament suspension generally has a larger magnetic susceptibility than the system of unlinked nanoparticles with the same average particle concentration. However, actual susceptibility gain strongly depends on length and flexibility of filaments. It is also shown that in a strong gravitational (centrifugal) field sedimentation profiles of filaments are less homogeneous than that of unlinked particles. The spatial distribution of filaments weakly depends on the intensity of interparticle dipole-dipole interactions.

Keywords: magnetic filaments, nanochains, ferrofluid, magnetic susceptibility, sedimentation equilibrium

1. Introduction

A magnetic filament is a chain of magnetic micro- or nanoparticles permanently connected by polymer linkers [1, 2]. Such filaments have numerous potential applications. Chains of magnetic particles can be used as self-propelling devices for drug and cargo delivery, as magnetically controlled microfluidic mixers and as micromechanical sensors [3, 4, 5, 6]. In Ref. [7], a suspension of nanosized magnetic filaments was proposed as an improved substitute for conventional ferrofluids, i.e. colloidal dispersions of unlinked monodomain nanoparticles in a nonmagnetic carrier liquid. Permanent chains are expected to have a strong response to magnetic field and a high resistance to shear stress, which can be a benefit in ferrofluid applications. Much effort has been recently devoted to the analytical and numerical study of suspended nanosized filaments in the limit of infinite dilution, when interaction between individual chains can be neglected [2, 7, 8]. In Ref. [9], a pair of interacting filaments was considered. However, large ensembles of interacting filaments, which are a closer approximation for filament-based ferrofluids, have not been thoroughly studied yet. In the present work, equilibrium properties of moderately concentrated filament suspensions are numerically investigated via the Langevin dynamics simulation method.

2. Model and simulation method

The simulated system consists of N_f filaments and each filament consists of equal number of particles l_f . So, the

total number of particles in the system is $N_p = N_f \cdot l_f$. Particles are uniformly magnetized spheres of equal diameter d and with magnetic moments of equal constant magnitude μ . The movement of the i th particle in the carrier liquid obeys the Langevin equations

$$\dot{\mathbf{v}}_i^* = -\partial U_i^* / \partial \mathbf{r}_i^* - \gamma^{*T} \mathbf{v}_i^* + \boldsymbol{\eta}_i^{*T}, \quad (1)$$

$$J^* \dot{\boldsymbol{\omega}}_i^* = -\hat{\boldsymbol{\mu}}_i \times \partial U_i^* / \partial \hat{\boldsymbol{\mu}}_i - \gamma^{*R} \boldsymbol{\omega}_i^* + \boldsymbol{\eta}_i^{*R}, \quad (2)$$

where asterisk denotes reduced quantities, d is used as a unit of length, particle mass m – as a unit of mass and the thermal energy $k_B T$ – as a unit of energy. Thus, $\mathbf{v}_i^* = \mathbf{v}_i \sqrt{m/k_B T}$ and $\boldsymbol{\omega}_i^* = \boldsymbol{\omega}_i \sqrt{md^2/k_B T}$ are the reduced linear and angular velocities, correspondingly, $\mathbf{r}_i^* = \mathbf{r}_i/d$ is the reduced particle position, $\hat{\boldsymbol{\mu}}_i = \boldsymbol{\mu}_i^*/\mu^* = \boldsymbol{\mu}_i/\mu$ is the unit vector along the particle magnetic moment, $\mu^* = \mu \sqrt{\mu_0/4\pi d^3 k_B T}$ is the reduced magnetic moment, μ_0 is the magnetic constant, $U_i^* = U_i/k_B T$ is the reduced particle potential energy, $J^* = J/md^2$ is the reduced moment of inertia, $\gamma^{*T} = \gamma^T \sqrt{d^2/mk_B T}$ and $\gamma^{*R} = \gamma^R \sqrt{1/d^2 mk_B T}$ are the reduced translational and rotational friction coefficients, $\boldsymbol{\eta}_i^{*T}$ and $\boldsymbol{\eta}_i^{*R}$ are the random Gaussian force and torque, which have zero mean values and satisfy the standard fluctuation-dissipation relationship

$$\langle \eta_{i\alpha}^{*T(R)}(t_1^*) \eta_{j\beta}^{*T(R)}(t_2^*) \rangle = 2\gamma^{*T(R)} \delta_{\alpha\beta} \delta_{ij} \delta^*(t_1^* - t_2^*), \quad (3)$$

the reduced time is $t^* = t \sqrt{k_B T/md^2}$.

The interaction energy of two arbitrary particles i and j consists of the steric repulsion energy $u_{sr}(i, j)$ and the

*Corresponding author

Email address: kuznetsov.a@icmm.ru (Andrey A. Kuznetsov)

dipole-dipole interaction energy $u_{dd}(i, j)$:

$$u_{sr}(i, j) = \begin{cases} u_{LJ}(r_{ij}) - u_{LJ}(r_{cut}), & r_{ij} < r_{cut} \\ 0, & r_{ij} \geq r_{cut}, \end{cases} \quad (4)$$

$$u_{LJ}(r) = 4\epsilon \left[\left(\frac{d}{r}\right)^{12} - \left(\frac{d}{r}\right)^6 \right], \quad (5)$$

$$u_{dd}(i, j) = \frac{\mu_0}{4\pi} \left[\frac{\boldsymbol{\mu}_i \cdot \boldsymbol{\mu}_j}{r_{ij}^3} - \frac{3(\boldsymbol{\mu}_i \cdot \mathbf{r}_{ij})(\boldsymbol{\mu}_j \cdot \mathbf{r}_{ij})}{r_{ij}^5} \right], \quad (6)$$

where u_{LJ} is the Lennard-Jones potential, $r_{cut} = 2^{1/6}d$ is the cutoff radius [10]. Additionally, some bonding interaction between adjacent particles in the filament must be imposed to preserve filament's chain-like structure. For this purpose, the phenomenological potential introduced in Refs. [2, 7] is used:

$$u_{bond}(i+1, i) = \frac{K}{2} \left[\mathbf{r}_{i+1, i} - \frac{(\hat{\boldsymbol{\mu}}_{i+1} + \hat{\boldsymbol{\mu}}_i)d}{2} \right]^2. \quad (7)$$

The potential mimics the harmonic spring that links opposite poles of two consequent particles in the filament. It is not only forbids neighbors to move too far from each other, but also promotes an alignment of their magnetic moments (it is implied that the magnetic anisotropy of particles is large and moments are ‘‘frozen’’ within the particle bodies). Three dimensionless energy parameters can be introduced for the simulated system: the steric repulsion parameter $\epsilon = \epsilon/k_B T$, the dipolar coupling parameter $\lambda = (\mu_0/4\pi)\mu^2/d^3 k_B T = \mu^{*2}$ and the elastic parameter $\varkappa = Kd^2/2k_B T$. Using these parameters, interaction potentials (4)–(7) can be rewritten in the reduced form:

$$u_{sr}^*(i, j) = \begin{cases} 4\epsilon \left(\frac{1}{r_{ij}^{*12}} - \frac{1}{r_{ij}^{*6}} + \frac{1}{4} \right), & r_{ij}^* < r_{cut}^* \\ 0, & r_{ij}^* \geq r_{cut}^*, \end{cases} \quad (8)$$

$$u_{dd}^*(i, j) = \lambda \left[\frac{\hat{\boldsymbol{\mu}}_i \cdot \hat{\boldsymbol{\mu}}_j}{r_{ij}^{*3}} - \frac{3(\hat{\boldsymbol{\mu}}_i \cdot \mathbf{r}_{ij}^*)(\hat{\boldsymbol{\mu}}_j \cdot \mathbf{r}_{ij}^*)}{r_{ij}^{*5}} \right], \quad (9)$$

$$u_{bond}^*(i+1, i) = \varkappa \left[\mathbf{r}_{i+1, i}^* - \frac{\hat{\boldsymbol{\mu}}_{i+1} + \hat{\boldsymbol{\mu}}_i}{2} \right]^2. \quad (10)$$

The input parameters of the simulation are \varkappa , λ , l_f , N_p and the average particle volume fraction $\bar{\varphi} = N_p \nu / V$, where $\nu = \pi d^3/6$ is the particle volume, V is the volume of the simulation cell. Other parameters are fixed: $\epsilon = 0.67$, $J^* = 0.1$, $\gamma^{*R} = 3$, $\gamma^{*T} = 1$. $\epsilon = 0.67$ ensures that at $\varkappa = 0$ and $\lambda = 0$ the system free energy coincides with the free energy of the ensemble of hard spheres with a diameter d [11]. Surely, in a more general case, when $\lambda > 0$ or $\varkappa > 0$, equilibrium properties of filaments will still depend on the particular choice of the steric repulsion potential. The usage of the ‘‘soft sphere’’ potential Eq. (8) in the present study is physically grounded since in most cases particles are stabilized by soft polymer shells [7]. Langevin equations are integrated using the modified leapfrog algorithm by Grønbech-Jensen and Farago [12].

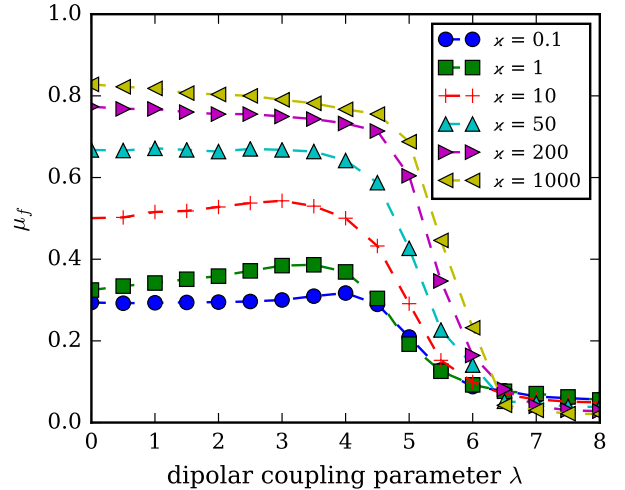


Figure 1: Average normalized magnetic moment of the isolated filament vs. the dipolar coupling parameter at different values of the elastic parameter \varkappa . $N_f = 1$, $l_f = 10$.

3. Results

3.1. Filament configuration at infinite dilution: effect of the elastic parameter

Auxiliary simulations were conducted in order to analyze the effect of the elastic parameter \varkappa on the behavior of the considered filament model. A single isolated ten-particle filament ($N_f = 1$, $l_f = 10$) was simulated in the absence of external force fields and under open boundary conditions (similarly to Refs. [2, 7]). Normalized average magnetic moment of the filament

$$\mu_f = \frac{1}{l_f \mu} \left\langle \left| \sum_{i=1}^{l_f} \boldsymbol{\mu}_i \right| \right\rangle \quad (11)$$

was calculated for different values of λ and \varkappa . Results are shown in Fig. 1. Let's first consider $\lambda = 0$. In this limiting case, dipole-dipole interactions between cross-linked nanoparticles are negligible. It is possible, for example, when particles have thick polymer shells with a characteristic diameter $d \gg d_c = [(\mu_0/4\pi)\mu^2/k_B T]^{1/3}$. At $\varkappa = 0.1$ $\mu_f \simeq 1/\sqrt{l_f} \simeq 0.3$, which coincides with the average magnetic moment of l_f independently fluctuating dipoles. As seen in Fig. 2(a), particles are chaotically moving in the proximity of each other and do not resemble a chain. An increase of \varkappa by two orders of magnitude increases magnetic moment only up to $\mu_f \simeq 0.5$. At this point the system obtains the chain-like structure, but the chain is rather flexible (see Fig. 2(b)). At $\varkappa = 10^3$ (Fig. 2(c)) $\mu_f \gtrsim 0.8$, which is close to the magnetic moment of a rigid rodlike chain ($\mu_f = 1$). At $\lambda \lesssim 4$ the magnetic moment only slightly depends on the dipolar parameter, but at $4 \lesssim \lambda \lesssim 6$ it rapidly decreases. At $\lambda > 6$ filaments are in the stable ring configuration with $\mu_f < 0.1$ (Fig. 2(d)). The ring formation occurs regardless the elastic parameter. In what follows only systems with $\lambda < 4$ will be

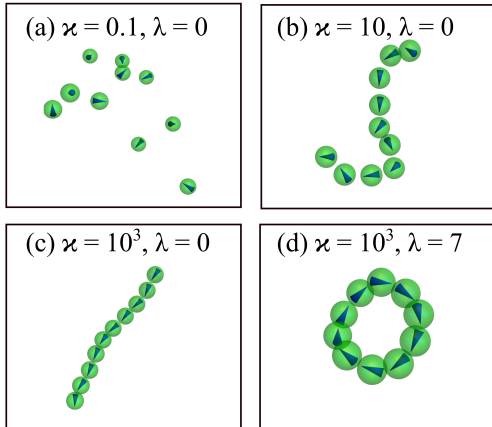


Figure 2: 3D snapshots of the isolated filament at different values of elastic (κ) and dipolar coupling (λ) parameters. $N_f = 1$, $l_f = 10$.

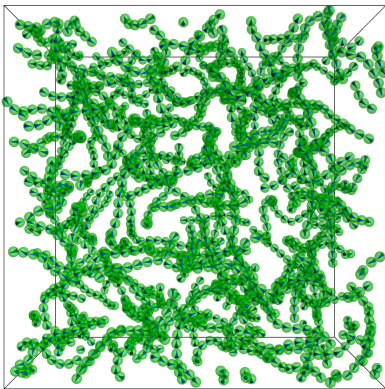


Figure 3: Snapshot of the filament ensemble inside the cubic box with 3D periodic boundary conditions. $N_p = 2000$, $\bar{\varphi} = 0.025$, $l_f = 10$, $\lambda = 2$, $\kappa = 10^3$.

considered since rings are known to weaken the magnetic response of ferrofluids [13].

3.2. Initial magnetic susceptibility of the filament suspension

To calculate the magnetic susceptibility of the filament suspension, the system of $N_p = 2000$ particles in the cubic cell with 3D periodic boundary conditions was simulated. Standard Ewald summation technique with “conducting” boundary conditions was used to calculate dipole-dipole interactions in the periodic system [10]. External fields were absent. Figure 3 shows an example of the system equilibrium configuration. Susceptibility was calculated as follows [14]:

$$\chi = \chi_L \left\langle \left(\sum_{i=1}^{N_p} \boldsymbol{\mu}_i \right)^2 \right\rangle \frac{1}{\mu^2 N_p}, \quad (12)$$

where $\chi_L = 8\lambda\bar{\varphi}$ is the Langevin susceptibility. In Fig. 4 concentration dependencies of χ are given for $\lambda = 2$, $\kappa =$

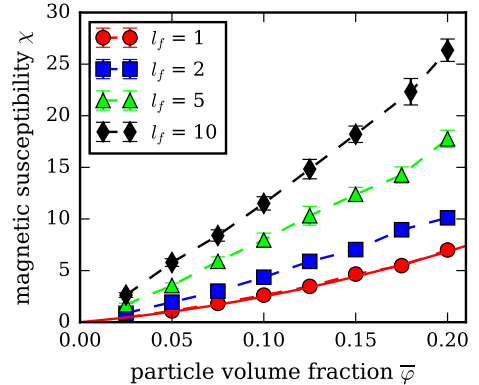


Figure 4: Initial susceptibility of the filament ensemble vs. the average particle volume fraction at different filament lengths. Solid curve is from Eq. (13). $N_p = 2000$, $\lambda = 2$, $\kappa = 10^3$.

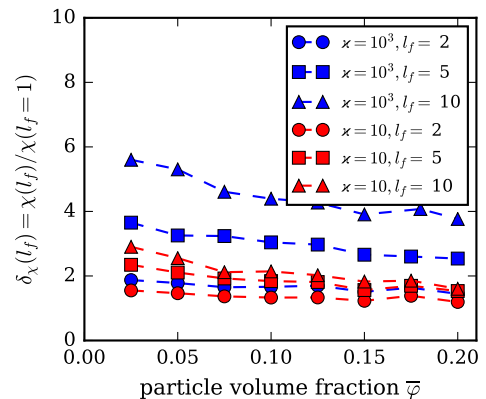


Figure 5: Susceptibility gain due to replacement of individual particles in the suspension with filaments vs. the average particle volume fraction. $N_p = 2000$, $\lambda = 2$.

10^3 and different filament sizes l_f . For $l_f = 1$, i.e. when particles are not forced to form chains, results are well described by the second-order modified mean-field model [15]

$$\chi = \chi_L (1 + \chi_L/3 + \chi_L^2/144). \quad (13)$$

For $l_f > 1$ susceptibility is expectedly larger. Figure 5 shows concentration dependencies of the quantity $\delta_\chi(l_f) = \chi(l_f)/\chi(l_f = 1)$. Basically, this quantity indicates how the replacement of individual colloidal particles with filaments increases the suspension magnetic response, if the amount of magnetic phase, its average concentration and the dipolar coupling parameter remain unchanged. It is seen that for flexible filaments ($\kappa = 10$) δ_χ weakly increases with the filament size, in a broad range of concentrations $\delta_\chi \lesssim 2$ regardless l_f value. For stiff chains ($\kappa = 10^3$) a much stronger increase of the susceptibility can be achieved. Though even in this case $\delta_\chi(l_f) < l_f$. It also seems that for fixed λ and l_f the quantity δ_χ decreases with the growth of the average particle concentration. To clarify this effect, further investigations are required.

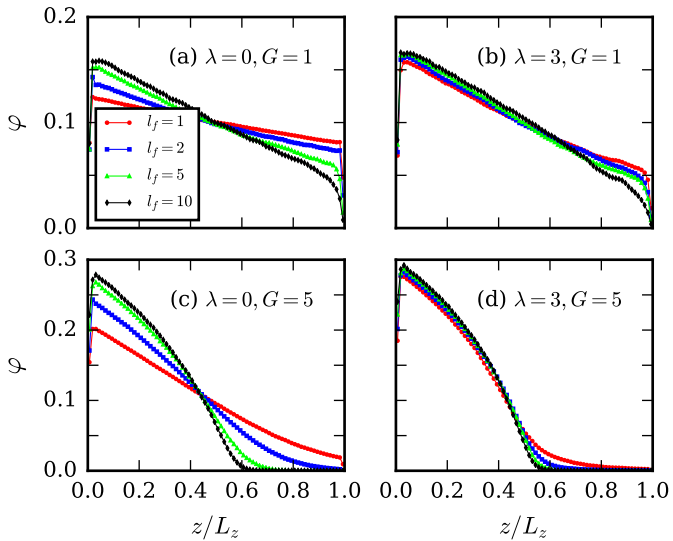


Figure 6: Sedimentation profiles of filaments with different lengths at different values of the dipolar coupling parameter (λ) and the gravitational parameter ($G = L_z/L_{sed}$). $N_p = 2000$, $\bar{\varphi} = 0.1$, $L_z = 80d$, $\varepsilon = 10^3$.

3.3. Sedimentation stability of the filament suspension

From an applied point of view, one of the most important characteristics of ferrofluids is their ability to maintain spatial homogeneity under the action of applied force fields such as gravitational or gradient magnetic ones [16]. To evaluate the stability of the filament-based ferrofluid, the process of filaments' sedimentation in a strong gravitational (centrifugal) field was simulated.

Simulation algorithm proposed in Ref. [11] was used. Filaments were placed inside the elongated rectangular cavity of the height L_z , gravitational field \mathbf{g} was acting along the cavity long axis (z -axis). Top and bottom surfaces of the cavity ($z = L_z$ and $z = 0$, correspondingly) were impenetrable for particles and 2D periodic boundary conditions were imposed along the x - and y - directions. To take into account the presence of the gravitational field, additional term in the i th particle's full energy was introduced: $u_g(i)/k_B T = z_i/L_{sed}$, where $L_{sed} = k_B T/\Delta\rho v g$ is the particle sedimentation length, $\Delta\rho$ is the density difference between the particle and the carrier liquid. Long-range dipole-dipole interactions were calculated using the modified Ewald summation technique adapted for the slab geometry. Details can be found in Ref. [17]. The main simulation result is the equilibrium concentration profile $\varphi = \varphi(z)$, where φ is the *local* volume fraction of particles at the height z .

Profiles obtained at different values of l_f , λ and the gravitational parameter $G = L_z/L_{sed}$ are given in Fig. 6. It is seen that at $\lambda = 0$ the suspension with $l_f = 10$ is substantially more inhomogeneous than the suspension with $l_f = 1$. It simply means that the gradient diffusion coefficient of stiff chains is lower than that of unlinked soft spheres. In the case of ten-particle filaments, profiles do

not significantly change with the growth of λ . On the contrary, the spatial homogeneity of unlinked particles is strongly affected by dipole-dipole interactions. At $\lambda = 3$ profiles for $l_f = 1$ and $l_f = 10$ become very close. This is probably due to the fact that at high λ magnetic particles tend to assemble into various aggregates even without polymer linkers [13].

4. Conclusion

It was numerically investigated how the replacement of individual nanoparticles with nanosized magnetic filaments will affect the equilibrium properties of ferrofluids. It was shown that at the same average concentration of magnetic phase the filament suspension have a stronger magnetic response than the standard ferrofluid. However, to obtain a large susceptibility gain (more than twofold), several requirements must be met. Filaments must not only be long, they have to be rather stiff: the characteristic energy of the polymer bonding between two adjacent particles in the filament must be several orders of magnitude larger than the thermal energy. The replacement of particles with filaments has a negative impact on the suspension stability in strong gravitational (centrifugal) fields. At high dipolar coupling parameters λ the effect is weak: concentration profiles for unlinked particles (monomers) and for the system of ten-particle filaments are almost the same. In both cases, magnetic phase distribution can be highly inhomogeneous. But the inhomogeneity of monomers decreases with decreasing λ , whereas for long filaments the suspension remains segregated even when dipole-dipole interactions are weak.

Obtained results suggest that the replacement of individual particles with filaments will have a greater impact on the system susceptibility if the average particle concentration is low. It means that interchain interactions (steric and/or dipole-dipole ones) are able to reduce the advantages of magnetic filament suspensions over standard ferrofluids. The exact mechanism behind this effect is not clear. Perhaps, a detailed study of filaments' microstructure at different concentrations will shed light on the problem. Another issue that deserves a special consideration is the stability of filament suspensions in high-gradient magnetic fields, which are typical for some applications of ferrofluids [16, 18]. These problems will be addressed in future articles.

5. Acknowledgments

The work was supported by the Foundation for Assistance to Small Innovative Enterprises in Science and Technology (agreement No. 8954GU/2015).

References

- [1] A. Čebers, Flexible magnetic filaments, *Curr. Opin. Colloid Interface Sci.* 10 (3) (2005) 167–175. doi:10.1016/j.cocis.2005.07.002.

- [2] J. J. Cerdà, P. A. Sánchez, C. Holm, T. Sintes, Phase diagram for a single flexible stockmayer polymer at zero field, *Soft Matter* 9 (29) (2013) 7185–7195. doi:10.1039/c3sm50278c.
- [3] C. Goubault, P. Jop, M. Fermigier, J. Baudry, E. Bertrand, J. Bibette, Flexible magnetic filaments as micromechanical sensors, *Phys. Rev. Lett.* 91 (26) (2003) 260802. doi:10.1103/physrevlett.91.260802.
- [4] R. Dreyfus, J. Baudry, M. L. Roper, M. Fermigier, H. A. Stone, J. Bibette, Microscopic artificial swimmers, *Nature* 437 (7060) (2005) 862–865. doi:10.1038/nature04090.
- [5] H. Wang, Y. Yu, Y. Sun, Q. Chen, Magnetic nanochains: a review, *Nano* 6 (01) (2011) 1–17. doi:10.1142/s1793292011002305.
- [6] A. Cebers, K. Erglis, Flexible magnetic filaments and their applications, *Adv. Funct. Mater.* 26 (22) (2016) 3783–3795. doi:10.1002/adfm.201502696.
- [7] P. A. Sánchez, J. J. Cerdà, T. M. Sintes, A. O. Ivanov, S. S. Kantorovich, The effect of links on the interparticle dipolar correlations in supramolecular magnetic filaments, *Soft Matter* 11 (15) (2015) 2963–2972. doi:10.1039/c5sm00172b.
- [8] J. J. Cerdà, P. A. Sánchez, D. Lüsebrink, S. Kantorovich, T. Sintes, Flexible magnetic filaments under the influence of external magnetic fields in the limit of infinite dilution, *Phys. Chem. Chem. Phys.* 18 (18) (2016) 12616–12625. doi:10.1039/c6cp00923a.
- [9] E. V. Novak, D. A. Rozhkov, P. A. Sanchez, S. S. Kantorovich, Self-assembly of designed supramolecular magnetic filaments of different shapes, *J. Magn. Magn. Mater.* 431 (2017) 152–156. doi:10.1016/j.jmmm.2016.10.046.
- [10] M. P. Allen, D. J. Tildesley, *Computer simulation of liquids*, Clarendon Press, Oxford, 1987.
- [11] A. A. Kuznetsov, A. F. Pshenichnikov, Sedimentation equilibrium of magnetic nanoparticles with strong dipole-dipole interactions, *Phys. Rev. E* 95 (3) (2017) 032609. doi:10.1103/physreve.95.032609.
- [12] N. Grønbech-Jensen, N. R. Hayre, O. Farago, Application of the g-jf discrete-time thermostat for fast and accurate molecular simulations, *Comput. Phys. Commun.* 185 (2) (2014) 524–527. doi:10.1016/j.cpc.2013.10.006.
- [13] S. S. Kantorovich, A. O. Ivanov, L. Rovigatti, J. M. Tavares, F. Sciortino, Nonmonotonic magnetic susceptibility of dipolar hard-spheres at low temperature and density, *Phys. Rev. Lett.* 110 (14) (2013) 148306. doi:10.1103/physrevlett.110.148306.
- [14] S. W. De Leeuw, J. W. Perram, E. R. Smith, Computer simulation of the static dielectric constant of systems with permanent electric dipoles, *Annu. Rev. Phys. Chem.* 37 (1) (1986) 245–270. doi:10.1146/annurev.physchem.37.1.245.
- [15] A. O. Ivanov, O. B. Kuznetsova, Magnetic properties of dense ferrofluids: an influence of interparticle correlations, *Phys. Rev. E* 64 (4) (2001) 041405. doi:10.1103/physreve.64.041405.
- [16] A. F. Pshenichnikov, A. V. Lebedev, A. V. Radionov, D. Efremov, A magnetic fluid for operation in strong gradient fields, *Colloid J.* 77 (2) (2015) 196–201. doi:10.1134/s1061933x15020155.
- [17] S. H. L. Klapp, M. Schoen, Spontaneous orientational order in confined dipolar fluid films, *J. Chem. Phys.* 117 (17) (2002) 8050–8062. doi:10.1063/1.1512282.
- [18] M. S. Krakov, I. V. Nikiforov, Effect of diffusion of magnetic particles on the parameters of the magnetic fluid seal: A numerical simulation, *Magnetohydrodynamics* 50 (1) (2014) 35–43. URL <http://mhd.sal.lv/contents/2014/1/MG.50.1.5.R.html>